Journal of Molecular Structure 1100 (2015) 366–375

Contents lists available at ScienceDirect

Journal of Molecular Structure

journal homepage: http://www.elsevier.com/locate/molstruc

DFT vibrational assignments, *in vitro* antifungal activity, genotoxic and acute toxicity determinations of the $[Zn(phen)_2(cnge)(H_2O)](NO_3)_2 \cdot H_2O$ complex

Juan J. Martínez Medina [a], Carola A. Torres [a], Walter S. Alegre [a], Carlos A. Franca [b], Libertad L. López Tévez [a], Evelina G. Ferrer [b], Nora B. Okulik [a], Patricia A.M. Williams [b, *]

[a] *Universidad Nacional del Chaco Austral, Cte. Fernández 755, 3700, Roque Sáenz Peña, Chaco, Argentina*
[b] *CEQUINOR, Dpto. de Química, Facultad de Ciencias Exactas, UNLP. 47 y 115, 1900, La Plata, Argentina*

ARTICLE INFO

Article history:
Received 27 April 2015
Received in revised form
28 July 2015
Accepted 29 July 2015
Available online 31 July 2015

Keywords:
Phenanthroline
Cyanoguanidine tautomers
Zinc complex
DFT calculations
Antifungal properties
Ames and *Artemia salina* tests

ABSTRACT

Calculations based on density functional methods were carried out for the $[Zn(phen)_2(cnge)(H_2O)](NO_3)_2 \cdot H_2O$ complex taking into account the presence of two different conformers for the cyanoguanidine ligand. The calculated geometrical parameters and the vibrational IR and Raman spectra were in agreement with the experimental data. On the other hand, the activities of the complex, the ligands and the metal against fungal strains have been measured. The complexation increased the antifungal activity of the metal and the ligand cyanoguanidine, and slightly decreased the antifungal activity of the ligand 1,10-phenanthroline against *Candida albicans*, *C. albicans* ATCC 10231 and *Candida krusei* (not against the others strains of Candida). The ligand 1,10-phenanthroline and the zinc complex showed in some cases higher activity than the common antifungal drug fluconazole. The complexation also increased the post-antifungal effect in the tested strains, except for *Candida parapsilosis*, even with a better efficiency than those of some conventional antifungal agents. Antifungal studies were coupled with safety evaluations using the *Artemia salina* and the Ames tests. The zinc complex behaved as a non-mutagenic and non-toxic compound at the tested concentrations. Moreover, the zinc complex could be safer than the ligand when used as an antifungal agent. Therefore, the interaction of zinc(II) with N-containing ligands may provide a promising strategy for the development of novel and more secure drugs with antifungal activity.

1. Introduction

Cyanoguanidine (cnge) has been widely employed as a ligand of the transition metals in the synthesis of coordination compounds [1,2]. Its solid state structure has raised several theoretical and experimental studies suggesting the coexistence of two tautomeric forms: cyanoimine and cyanoamine [3] (Scheme 1).

Despite its biological importance, cnge has also commercial applications as an intermediate in the formation of pharmaceuticals, pesticides, fungicides, and various polymers. Some transition metal ions (i.e. copper, platinum and nickel) are able to catalyze the addition of alcohols to the nitrile group in cnge, forming n-alkylguanylureas that coordinates the metal ions [4–7]. On the other hand, 1,10-phenanthroline (phen) can act as a strong field bidentate ligand that forms very stable chelates with many transition metals of the first row [8]. This molecule has antibacterial, antifungal and antiviral properties [9]. Besides, it is well known that zinc is an essential metal, widely distributed in cells, and is the most abundant intracellular trace element. Catalytic, structural, and regulatory are the main biological roles played by the biometal [10].

The development of resistant strains is increasing as a result of excessive antibiotic use. In this context, it is interesting to note the enormous importance of developing novel antimicrobial drugs for the treatment of infectious diseases [11,12]. The antimicrobial action of phen has been demonstrated on several bacterial and fungal strains [13,14]. Zinc is an essential element involved in many vital cellular reactions at its low endogenous concentrations. When the concentrations of Zn(II) ion became higher than the optimal range, the ions can enter inside the microbial cells producing cytotoxic effects on the prokaryotic cells. The antimicrobial activity of Zn(II) is

* Corresponding author.
E-mail address: williams@quimica.unlp.edu.ar (P.A.M. Williams).

http://dx.doi.org/10.1016/j.molstruc.2015.07.061
0022-2860/

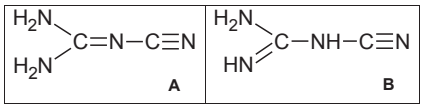

Scheme 1. Structures of cyanoimine (A) and cyanoamine (B).

essentially dependent on the microbial strain [15]. In this way, Zn(II) might be able to display its antimicrobial activity acting as either antibacterial or antifungal agent. Moreover, the antifungal profile of some compounds can be modified upon complexation with zinc ion [13,16–22]. These Zn(II) complexes exerts antifungal action against some Candida and others fungal strains, whereas other complexes like $[Zn(Hz_2DAP\text{-}2H)]\cdot H_2O$ (with Hz2DAP: bis(phthalazine-1-hydrazone)-2,6-diacetylpyridine) promotes the growth of *Candida albicans* [23].

In our previous paper [24], we reported the structural, spectral and potentiometric characterization, and the antibacterial activity of the $[Zn(phen)_2(cnge)(H_2O)](NO_3)_2\cdot H_2O$ complex. The X-ray structure of the complex reveals that the Zinc(II) ion is located in a distorted octahedral environment, coordinated to two nearly planar [*rms* deviation of atoms from the best least-squares plane less than 0.055 Å] bidentate and mutually perpendicular phen [dihedral angle of 88.82(3)°] [Zn–N bond lengths ranging from 2.124(2) Å to 2.193(2) Å]. The remaining two *cis*-positions are occupied by cyanide nitrogen of cnge [d(Zn–N) = 2.092(2) Å] that enters coordination slightly bent [∠ (Zn–N–C) = 161.1(2)°] and a water molecule [d(Zn–Ow) = 2.112(2) Å]. To extend this study, we report herein the calculations of the geometry and the vibrational behavior based on density functional theory (DFT) [25–27] and compared these results with the previous experimental data obtained by X-ray, FT-IR and FT-Raman measurements. We have also investigated the antifungal activity by the agar diffusion and the agar dilution methods and the post-antifungal effect (PAFE) for the Zn(II) ion, the ligands cnge and phen and the zinc complex against seven strains of Candida. The antifungal studies were coupled with the evaluation of the mutagenicity and acute toxicity of all compounds.

2. Experimental

2.1. Materials

All chemicals were of analytical grade. Anhydrous Zinc(II) chloride ($ZnCl_2$) was obtained from Merck, solvents and all the other analytical grade chemicals used were purchased from Sigma. The growth media (Mueller Hinton Broth and Mueller Hinton Agar) and blank sterile discs were purchased from Britannia and Bioartis, respectively. The zinc complex was prepared according to the preparative technique described in our previous report [24]. Electronic absorption spectra were recorded on a spectrophotometer Agilent Technologies (Cary 60 UV–vis).

2.2. Methods

2.2.1. Computational methodology

The X-ray diffraction data was employed as the starting structure to optimize the geometry of the zinc complex using tools from the DFT. Calculations were performed using the GAUSSIAN 09 program package [28]. Molecular structures of ligands and metallic complexes were fully optimized at various levels. Geometry optimization procedures were started from the experimental crystallographic data using the Beck three-parameters hybrid exchange-correlation functional, known as B3LYP [29] employing different basis set for different atoms. Theoretical calculations were carried out simulating water environment using the conducting polarizable continuous model (CPCM) as implemented in the software package [30]. Basis sets of triple-zeta quality with polarized (TZVP) functions for atoms of Zn, C and H, and a TZVP basis set with diffuse functions (TZVPD) for oxygen and nitrogen atoms [31].

IR absorption and Raman spectra of cnge in different physical states (crystalline, solutions and composition with porous glasses) reveals the co-existence of two different structural cnge species: cyanoimine and cyanoamine [3]. Theoretical studies of the cnge isomers confirm that these two forms co-exist at the same time [3,32]. Accordingly, it was suggested that the X-ray diffraction data showing equivalent C–N and C=N bond lengths in the guanidine fragment is a consequence of the superposition of both tautomers that are present simultaneously in cnge samples. Taking into account these findings, the cation complex geometry optimization was carried out considering both cyanoguanidine tautomers individually, 1-cyanoguanidine (cyanoamine) and 2-cyanoguanidine (cyanoimine). The structures of the zinc complexes optimized with cyanoamine and cyanoimine were called (**1**) and (**2**), respectively.

Vibrational spectroscopy is one of the most important and promising tools for the characterization of the structural features of molecules (backbone or functional groups). The combination of theoretical calculations with IR and Raman spectroscopies provide invaluable structural information [33]. Vibrational calculations at the same level of theory were performed to determine the consistency of the minimum in the potential energy surface and to assign the theoretical vibrational spectra.

Orthogonal rotations are commonly used for comparing macromolecular structures, and the root mean square deviation (RMSD) is a natural metric for the quantization of the similarity of two optimally rotated structures [34]. To test the validity of quantum chemical calculations in reproducing the experimental structure of the zinc complex RMSD between the coordinates of both macromolecules were calculated using Qmol package [35].

2.2.2. Stability studies

In order to evaluate that in the *in vitro* studies the effects observed by the dissolved complex are due to the complex itself and not to its dissociation products, stability studies of the zinc complex under the same conditions of antimicrobial and toxicological assays were performed. The dissolution has been carried out in distilled water and in artificial seawater. Stability determinations were followed spectrophotometrically (variation of the electronic absorption spectra with time) at least for 30 min that is the time of manipulation of the solid dissolved before it was employed in the different assays.

2.2.3. Antifungal assays

The antifungal profile of the metal ($ZnCl_2$), the ligands (cnge and phen) and the complex have been studied against seven fungal strains by two different microbiological methods (agar diffusion and agar dilution methods). PAFE measurements were performed by a spectrophotometric method [36].

Control strains for the agar diffusion and agar dilution methods included seven strains of Candida namely: *Candida parapsilosis* ATCC 22019, *C. albicans* ATCC 10231, and clinical isolates of *Candida tropicalis*, *Candida krusei*, *Candida glabrata*, *C. parapsilosis* and *C. albicans*. Mueller Hinton Broth (MHB) or Mueller Hinton Agar (MHA) have been used for the cultivation/assay medium for all strains. The inocula of fungal strains were prepared from 18 h-old broth cultures. A McFarland 0.5 suspension was prepared for each isolate (~10^8 colony forming units (CFU) per mL, CFU mL^{-1}) and employed in all assays [12,37].

Stock solutions were prepared at different concentrations for

the different assays. For the agar diffusion method, the zinc complex was dissolved in the mixture H_2O:DMSO (50:50) and the metal and ligands were dissolved in distilled water to a final concentration of 250 mmol L^{-1}. For the agar dilution method, all compounds were dissolved in distilled water, to a final concentration of 15 mg mL^{-1}. Serial two-fold water dilutions were performed from the stock solutions of antimicrobial agents to give concentrations ranging from 14.65 to 15000 μg mL^{-1}. For the analysis of PAFE, the ligand phen and the zinc complex were dissolved in distilled water to a final concentration of 234.30 μg mL^{-1}. For the toxicological assays, the ligand phen and the zinc complex were dissolved in artificial seawater to a final concentration of 1875 μg mL^{-1}. All solutions previously described were sterilized by filtration before use.

2.2.4. Agar diffusion method

As a preliminary screening, all compounds were tested against fungi for their inhibitory activity. A fungal suspension of turbidity equaled to 0.5 McFarland standard were uniformly spread using sterile cotton swabs on sterile Petri dishes containing MHA. Blank sterile discs of 6 mm in diameter were aseptically impregnated with 8 μL of the sterile solutions of each compound. The zinc complex was tested at a concentration of 1.34 mg/disc and phen, at 0.4 mg/disc. The discs were allowed to stand until complete solvent evaporation and applied on the surface of previously inoculated solid agar. The mixture H_2O:DMSO (50:50) was used as negative control. Fluconazole (0.04 mg/disc) was used as positive reference standard. The plates were incubated aerobically at 37 °C for 48 h. The diameters of inhibition zones were evaluated in millimeters. The values reported are an average of at least three independent experiments [12,37].

2.2.5. Agar dilution method

The minimum inhibitory concentration (MIC) of each compound was determined by this method. After preparation of serial two-fold water dilutions of the tested compounds, 0.5 mL of each dilution were added to 4.5 mL of melted MHA and poured into a Petri dish (45 × 15 mm). The final concentrations ranging in the MHA were from 1.46 to 1500 μg mL^{-1}. An agar plate without antimicrobial agent was established as a sterility and organism growth controls. After cooling and drying, the agar surface was inoculated with 2 μL of the fungal suspensions and incubated aerobically at 37 °C for 48 h. After incubation, MICs were interpreted and the inhibition of microbial growth was judged by comparison with growth in control plates. MIC values of fluconazole (positive reference standard) were determined. The MIC was defined as the lowest dilution of the complex that inhibited the visible growth of the test organism. A single colony or a faint haze caused by the inoculum should not be read as growth. Each MIC experiment was repeated three times [12,24,37–39].

2.2.6. Analysis of PAFE by spectrophotometry

Nevertheless, the MIC determination is an important antimicrobial assay to measure the susceptibility of some microorganisms against antimicrobial agents but provides limited information of the activity of the drug over time. In this context, the determination of PAFE was considered relevant to establish the possible modification of this pharmacodynamic parameter of the metal ion and the ligands upon complexation. The PAFE is the period of inhibition of fungal growth after the antifungal agent has been completely removed. This period can also be a measure of the delayed regrowth of fungi after a short period of antifungal exposure. The presence of PAFE may be an important consideration in designing antifungal dosage regimens and its determination is recommended in pre-clinical evaluation of all new antimicrobial agents [36,37].

In this *in vitro* study, a spectrophotometric method was used to investigate the PAFEs. Firstly, microcentrifuge tubes containing 900 μL of broth with the antimicrobial compound at twice the MIC value (2× MIC) were inoculated with 100 μL of a fungal suspension adjusted to 0.5 McFarland standard. Secondly, inoculated microcentrifuge tubes were placed in a water bath at 37 °C for an exposure period of 1 h. Thirdly, the antimicrobial agent was removed by dilution (1:1000) in a pre warmed antimicrobial-free medium. Finally, the diluted cultures were reincubated at 37 °C reading the transmittance at regular time intervals. Growth controls with inoculum but without the antimicrobial compounds were included with each experiment. These unexposed cultures underwent the same "drug removal" procedures as the exposed cultures. A 5% decrease in transmittance was used to define the point at which detection of growth occurred. The duration of PAFE was calculated by using the formula PAFE = T−C where T was the time required for a 5% decrease in transmittance for the antimicrobial-exposed organisms and C was the time required for the same inoculum in the control to decrease 5% in transmittance. Transmittance readings (670 nm) were recorded at 5 min intervals. Each PAFE measurement was carried out in duplicate [36,37].

2.2.7. Ames test

It is very important to investigate the mutagenic potential of the novel antimicrobial drugs because some chemical agents which show mutagenicity can induce cancer [40]. Mutagenicity of the ligand phen and the zinc complex was evaluated by the *Salmonella*/microsome assay that is based on the plate-incorporation method proposed by Maron and Ames [41], using two strains of *Salmonella typhimurium* (TA98 and TA100). The test strains were obtained from frozen culture and were grown overnight for 12–14 h at 37 °C in Mueller Hinton broth. The different concentrations of the ligand phen and the zinc complex (47, 24 and 12 μg/plate) were added to 2 ml of top agar mixed with 100 μl of bacterial culture (1–2 × 10^8 cells mL^{-1}) adding this mixture to a plate with minimal agar. These plates were incubated at 37 °C for 48 h and the number of His+ revertant colonies was counted. The concentrations employed in this assay were selected taking into account the MIC values for antifungal activity. All experiments were made in duplicate. The Mutagenic index (MI) was calculated as the average number of revertants per plate divided by the average number of revertants per plate from the negative control for each dose.

2.2.8. Artemia salina test

For determining the acute toxicity of the ligand phen and the zinc complex in brine shrimp, eggs of *A. salina* were incubated in a hatching chamber with artificial seawater at 20–30 °C (One liter of seawater contains: NaCl, 23 g; $MgCl_2.6H_2O$, 11 g; Na_2SO_4, 4 g; $CaCl_2.2H_2O$, 1.3 g; KCl, 0.7 g) [42] The pH was adjusted to 9.0 using Na_2CO_3 to avoid risk of death to the *Artemia* larvae by decrease of pH during incubation [43]. After 24 h, the larvae (nauplii) were extracted and counted using a micropipette. For the ligand phen and the zinc complex, five concentrations (in triplicate) were tested in order to determine dose–response relationship and negative (distilled water) and a positive ($K_2Cr_2O_7$) controls were used. Concentrations tested were 188, 94, 47, 24 and 12 μg mL^{-1}. These concentrations were selected taking into account the MIC values for antifungal activity. The wells containing the sample and 10 larvae of brine shrimp, including the control groups, were filled to a total volume of 100 μl with artificial seawater. After 24 h, live larvae were counted and the medium lethal concentration (LC50) value was estimated.

3. Results and discussion

3.1. DFT calculations

The geometries of the zinc complexes formed with both cyanoguanidine tautomers ((**1**) with cyanoamine and (**2**) with cyanoimine) were optimized without any constrains. The structures and atom labels of the [Zn(phen)$_2$(cyanoamine)H$_2$O] complex (**1**) and the [Zn(phen)$_2$(cyanoimine)H$_2$O] complex (**2**) are depicted in Figs. 1 and 2, respectively.

The selected optimized geometric parameters for the experimental structure in comparison of both complexes, (**1**) and (**2**), are gathered in Table 1. The whole data are listed in Supplementary material (Table S1).

The DFT-optimized structures converged successfully, in good agreement with the experimental X-ray one, implying the adequacy of the theoretical method employed for the geometry optimizations of this particular system. The Zn–N (cnge) distances are in agreement with the experimental values [24].

The general trends observed in the experimental data are well reproduced in the calculations. However, the comparison of the theoretical data with the experimental ones indicates that the optimized angle values are slightly different with the experimental determinations. It should be noted that the geometry of the solid state structure is subjected to intra and intermolecular interactions, such as hydrogen bonding and van der Waals interactions, whereas the calculations have been performed for isolated molecules. The optimized structures of the isolated complexes are superimposed on the crystallographic structures in Fig. 3.

The close structural relationship between the calculated and crystallographic observed structures is best illustrated with a RMS overlay error of 1.156 Å and 1.155 Å for (**1**) and (**2**), respectively, when the atoms of the coordination sphere of zinc are superimposed. The slightly higher values of RMS overlay error can be assigned to the fact that the X-ray structures were measured in a compacted crystalline form.

The theoretical IR and Raman spectra of the two complexes are shown in Fig. 4a, b and 5a, b and compared with the experimental one (Figs. 4d and 5d). Both calculated spectra showed a single band around 2200 cm^{-1} assigned to the C≡N stretching mode. The experimental stretching frequencies for the strong bands assigned to the coordinated cyano group were found to be located at 2189 cm^{-1} and 2148 cm^{-1} and have been assigned to the contribution of the two tautomers (**1**) and (**2**), respectively, present in the solid state (see below) [24]. Our calculated values of 2170 cm^{-1} (intensity, 803) and 2150 cm^{-1} (intensity, 1704) for (**1**) and (**2**), respectively, showed the same pattern than the experimental data. These results are in accordance with previous reports [3,32,44] and indicate the coexistence of two different complexes enclosing different tautomeric forms of cnge coordinated to the zinc center in the solid state, each one. The calculated bond lengths and angles are compatible with a higher contribution of (**2**) (Zn-cyanoimine) and the same behavior has been observed in the theoretical calculations of the imino tautomer of isolated cyanguanidine, the predominant form, which resulted energetically more stable by about 42–50 kJ than the amino form [44]. The calculations presented herein indicate that (**2**) (Zn-cyanoimine tautomer) is again more stable by 5.1 kJ/mol than the Zn-cyanoamine form (**1**). From Table 1 it is clear that the calculated results for cnge in (**2**) showed higher agreement with the experimental data than the theoretical values for (**1**). Nevertheless, to reproduce the experimental FTIR and FT-Raman spectra (in band position and intensities) a weight of the spectra for (**1**) and (**2**) of 70.67% and 29.33%, respectively, must be applied to show the doublet in the band corresponding to the C≡N stretching vibration (Figs. 4c and 5c). In summary, both, experimental and theoretical data regarding the vibrational spectra of the complex suggest the coexistence of both tautomeric forms of cnge coordinated to the Zn ion in the crystalline state.

Moreover, the nitrate stretching band in the experimental spectra of the complex, can be observed at 1380 cm^{-1} (FTIR, $\nu_3(E')$ mode) and 1055 cm^{-1} (Raman, $\nu_{1(}A'_1)$ mode). These bands are absent in the calculated spectra because the DFT calculations were

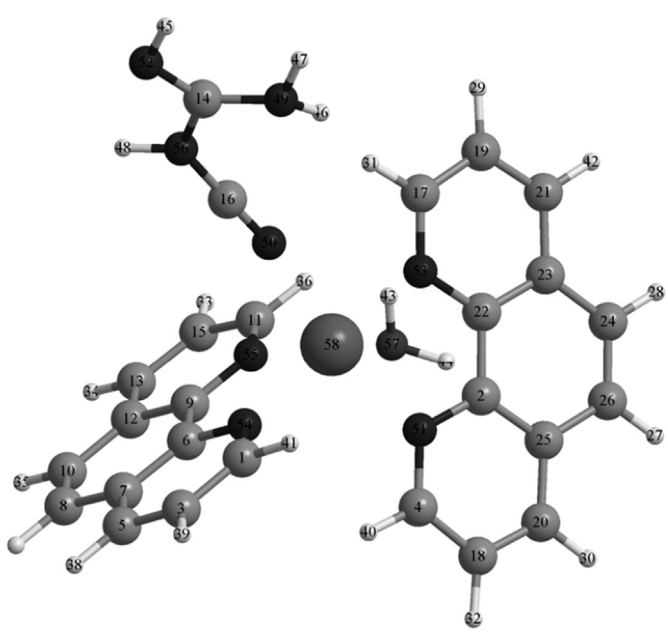

Fig. 1. Optimized geometry of (**1**) [Zn(phen)$_2$(cyanoamine)H$_2$O]. The black ball represents N atom the gray ball represents O atom and the light gray ball represents C atom. Atom 58 is Zn.

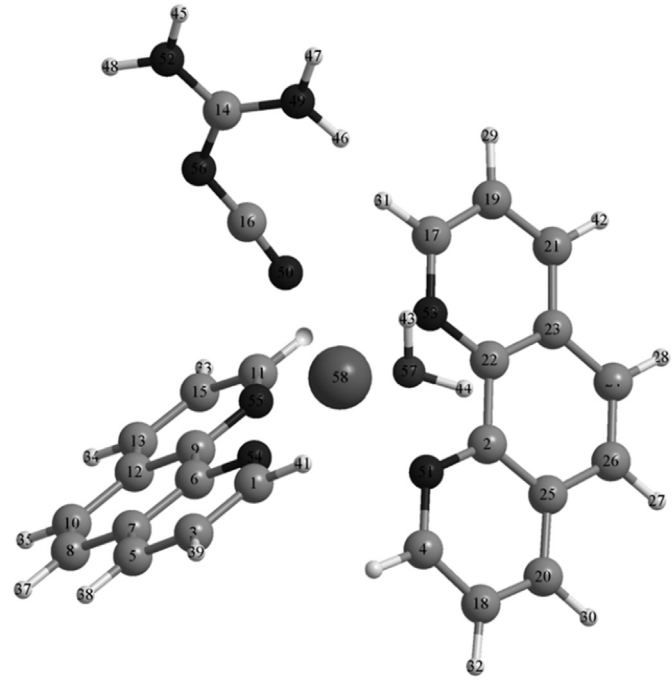

Fig. 2. Optimized geometry of (**2**) [Zn(phen)$_2$(cyanoimine)H$_2$O]. The black ball represents N atom the gray ball represents O atom and the light gray ball represents C atom. Atom 58 is Zn.

Table 1
Selected bond lengths (Å) and angles (°), around Zn and for cnge, calculated for (**1**) [Zn(phen)$_2$(cyanoamine)H$_2$O] and (**2**) [Zn(phen)$_2$(cyanoimine)H$_2$O]. Experimental values are reported for comparative purposes [24].

Bond lenghts[a]	Exp.	Calc.[b] 1	Calc.[c] 2	Bond angles[a]	Exp.	Calc.[b] 1	Calc.[c] 2
Zn(58)–N(53)	2.136	2.159	2.173	N(53)–Zn(58)–N(51)	77.15	77.6	76.5
Zn(58)–N(51)	2.189	2.184	2.215	N(54)–Zn(58)–N(55)	77.29	77.8	77.2
Zn(58)–N(55)	2.193	2.174	2.187	C(16)–N(50)–Zn(58)	161.1	168.3	169.9
Zn(58)–N(54)	2.124	2.158	2.177	N(49)–C(14)–N(52)	119.1	130.0	119.1
Zn(58)–O(57)	2.112	2.278	2.308	N(49)–C(14)–N(56)	123.3	114.4	123.8
Zn(58)–N(50)	2.092	2.211	2.102	C(14)–N(56)–C(16)	119.2	125.7	122.6
C(14)–N(49)	1.342	1.362	1.337	N(52)–C(14)–N(56)	117.5	115.6	117.0
C(14)–N(56)	1.345	1.423	1.334	N(50)–C(16)–N(56)	174.2	178.9	174.9
C(14)–N(52)	1.320	1.271	1.334				
C(16)–N(50)	1.164	1.155	1.166				
C(16)–N(56)	1.296	1.312	1.286				

[a] For the denomination of the atoms see Figs. 1 and 2.
[b] (**1**) Calculated at B3LYP/TZVPD.
[c] (**2**) Calculated at B3LYP/TZVPD.

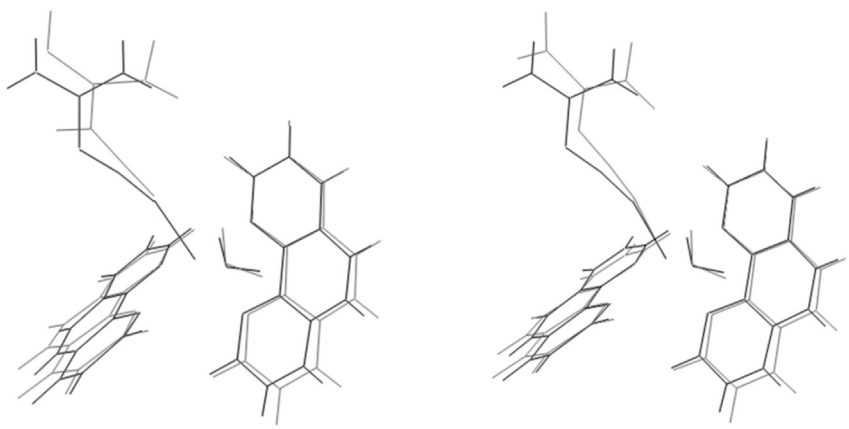

Fig. 3. Overlayed structures of the solid state (gray) and calculated (light gray) structures of (**1**) (left) and (**2**) (right).

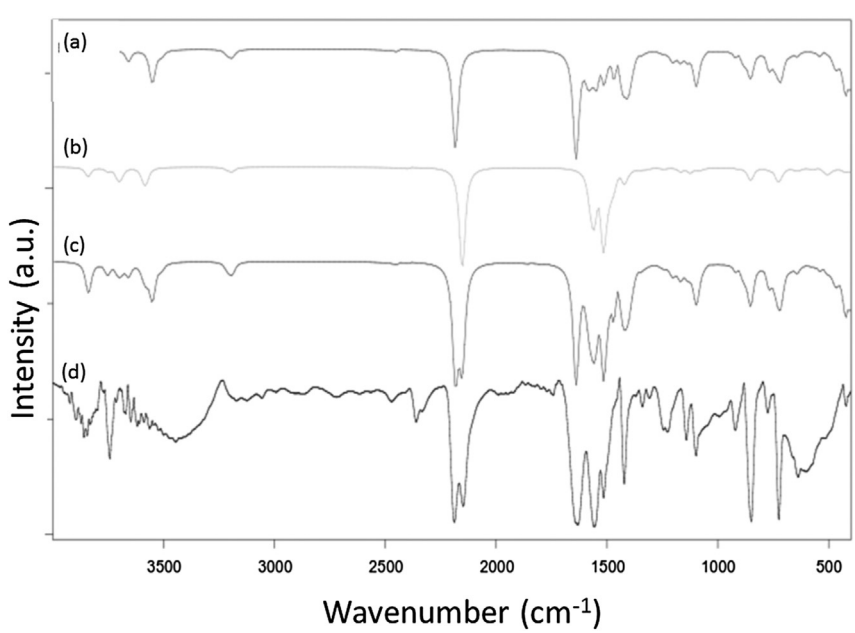

Fig. 4. Infrared spectra of (a) (**1**), (b) (**2**), (c) weighted spectrum ((**1**) and (**2**)) and, (d) experimental spectrum.

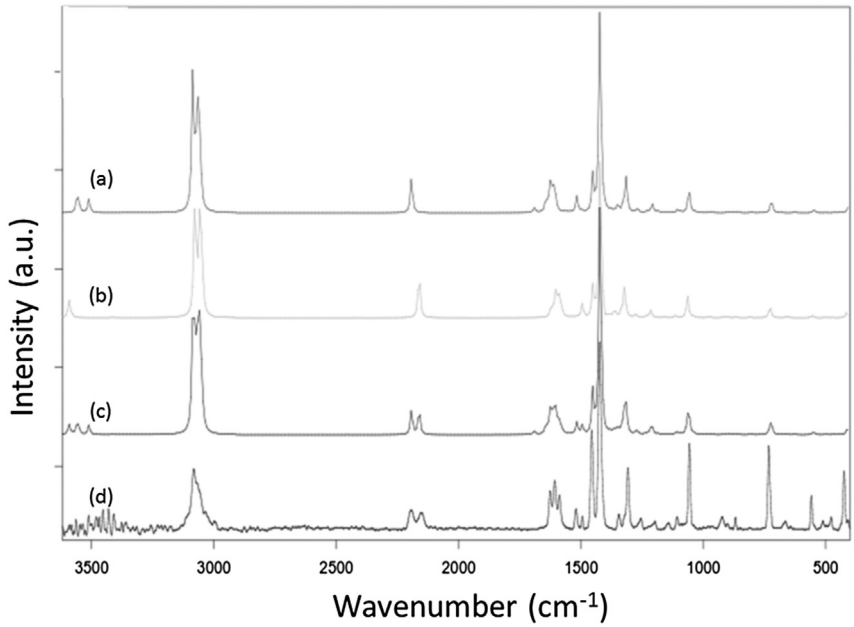

Fig. 5. Raman spectra of (a) (**1**), (b) (**2**), (c) weighted spectrum ((**1**) and (**2**)) and, (d) experimental spectrum.

only performed with the coordination complex in its cationic form.

3.2. Stability studies in solution

In a previous work [24], we have reported the stability of the ligands in aqueous solution and the stability of the zinc complex in the mixture H_2O:DMSO (50:50). Its stability under the experimental conditions of the antifungal and toxicological assays has been measured herein. The complex was dissolved in distilled water and in artificial seawater to a final concentration of 2.5×10^{-5} mol L^{-1}. The electronic absorption spectra of the zinc complex are displayed in Figs. 6 and 7. It can be seen that the solutions remained stable for at least 2 h being the zinc complex the only specie that contributes to the activity detected in the biological tests. The presence of the same bioactive solution species in all the tested dissolution media (H_2O:DMSO (50:50) [24], distilled water and artificial seawater) has been established allowing the determination that the complex remained without decomposition during the manipulation of the solutions for the biological tests (the manipulation time for the biological determinations was 30 min). This species corresponds to the complex named as $[ZnA_2LH]^{2+}$ (A = o-phen, LH = cnge) (according to the species distribution pattern) which is dominant in the pH range 4–9 [24].

4. Biological assays

4.1. Agar diffusion method

Results of this preliminary screening (Table 2) confirm the antimicrobial activity of the ligand phen and showed a similar effect of the zinc complex against all strains of Candida at the tested concentrations. The metal and the ligand cnge did not produce

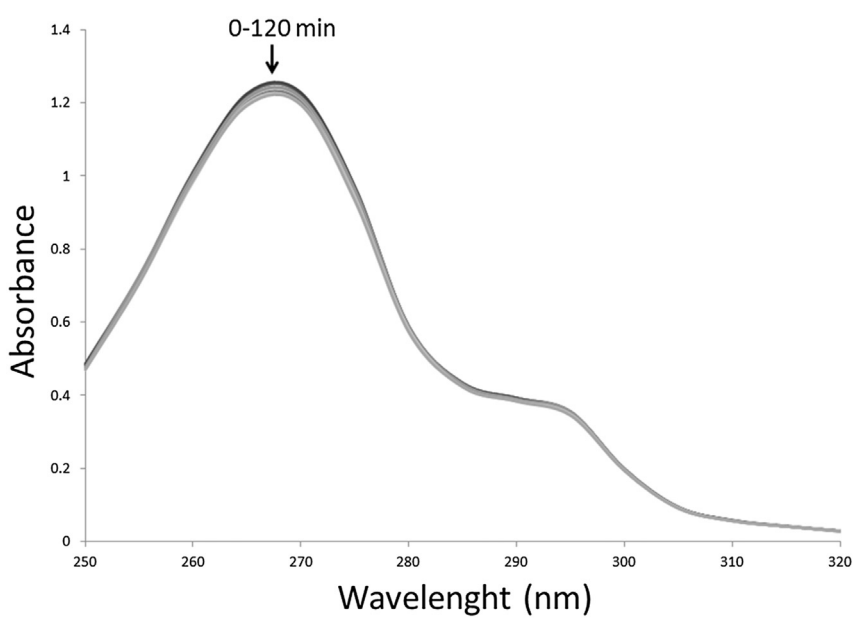

Fig. 6. Time variation of the electronic absorption spectra of the zinc complex in distilled water (2.5×10^{-5} mol L^{-1}), room temperature.

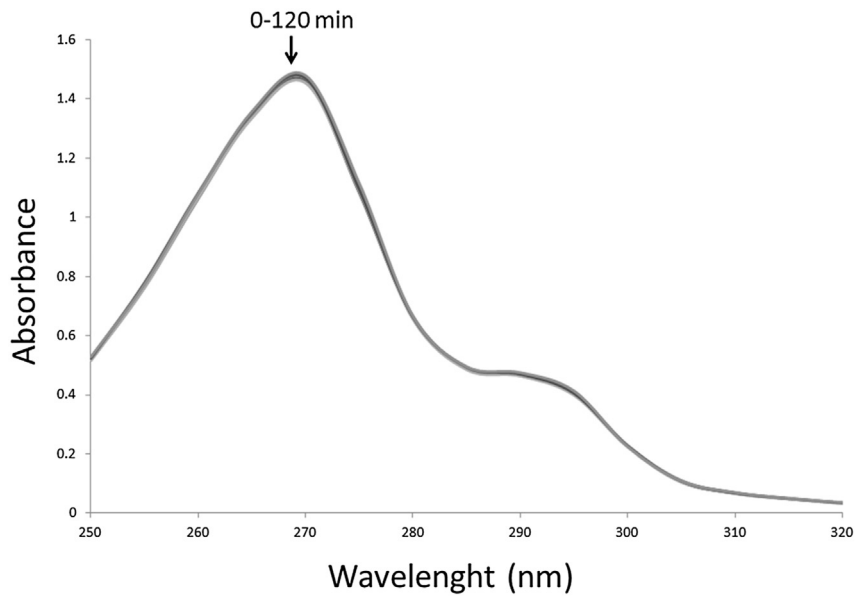

Fig. 7. Time variation of the electronic absorption spectra of the zinc complex in artificial seawater (2.5×10^{-5} mol L^{-1}), room temperature.

inhibition halos at the tested concentrations, suggesting no antifungal activity for these compounds. The observed order of zone of inhibition for the zinc complex decreased in the following order: *C. parapsilosis* > *C. tropicalis* > *C. albicans* ATCC > *C. glabrata* > *C. krusei* > *C. parapsilosis* ATCC > *C. albicans*.

The antifungal activity of several Zn(II) complexes against different strains of Candida was previously reported in the literature [16,17,22]. A similar order of inhibition zones of *C. parapsilosis* > *C. tropicalis* > *C. albicans* for the complex $[Zn(NAL)_2(N_3)_2]$ [16] (NAL: N-phenyl-3-pyridinecarboxamide) and *C. glabrata* > *C. albicans* for the complex $[ZnCl_2(3TTSCH)_2]$ [17] (3TTSCH: 3-thiophene aldehyde thiosemicarbazone), respectively, has been reported. In addition, the halos produced by the zinc complex were bigger than the halos reported by M. Montazerozohori et al. for a series of zinc halide/pseudohalide complexes of a bidentate Schiff base ligand against *C. albicans* [22].

4.2. Agar dilution method

The minimum inhibitory concentration (MIC) values of $ZnCl_2$, phen, the zinc complex and fluconazole as positive control are displayed in Table 3. In vitro measurements of antimicrobial activities with MIC values greater than 1000 μg mL^{-1} are considered with no relevance from a clinical perspective [37–39]. In this context, the antifungal activity of cnge against all tested strains (MIC > 1500 μg mL^{-1}) and the antifungal activity of the metal against *C. albicans*, *C. albicans* ATCC, *C. glabrata* and *C. krusei* (MIC = 1500 μg mL^{-1}) are no relevant. The antifungal activity of the metal against *C. parapsilosis*, *C. parapsilosis* ATCC and *C. tropicalis* was low (MIC = 750 μg mL^{-1}). These results were consistent with those observed in the preliminary screening.

Phenanthroline and its derivatives (including its metal complexes) are of great interest since they exhibit numerous biological activities such those against cancer and infections caused by virus, bacteria or fungi [9]. The MIC values of the free ligand phen against *C. albicans*, *C. albicans* ATCC and *C. krusei* were lower than those of the zinc complex. These results were consistent with those observed in the preliminary screening. Some of the previously reported MIC values of the ligand phen against different fungal strains were in agreement with our data [37].

It can be seen from Table 3 that the complexation increased the antifungal activity of the metal and the ligand cnge, and decreased the antifungal activity of the ligand phen against *C. albicans*, *C. albicans* ATCC *and C. krusei*. Nevertheless, the antifungal activity of phenanthroline was slightly lower than that of the complex (one order of magnitude in the dilution scale). The complexation didn't decrease the antifungal activity of the ligand phen against the others strains of Candida. The most interesting finding was that the zinc complex showed higher activity (lower MIC values) than fluconazole against *C. albicans*, *C. albicans* ATCC, *C. glabrata* and *C. krusei*. Taking into account the MIC values previously reported for some Zn(II) complexes against similar strains of Candida, we observed for the Zn/cnge/phen complex a better antifungal activity [13,18–21]. In a previous paper [37], we have reported the

Table 2
Preliminary screening of antimicrobial profile of the ligand phen, the zinc complex and fluconazole as positive control against the fungal strains. Diameters of zones of inhibition in mm. Diameters of zones of inhibition in mm. [phen]: 0.40 mg/disc [Zinc complex]: 1.34 mg/disc, [Fluconazole]: 0.04 mg/disc.

	Phen	Zinc complex	Fluconazole
C. albicans	59.3 ± 1.1[a]	13.7 ± 0.6	43.6 ± 1.5[a]
C. albicans ATCC	56.7 ± 2.9	52.7 ± 2.5	48.7 ± 1.5
C. parapsilosis	56.7 ± 5.8	59.3 ± 1.1	50.7 ± 1.1
C. parapsilosis ATCC	58.3 ± 1.5[a]	44.7 ± 2.5	39.6 ± 2.0[a]
C. tropicalis	43.3 ± 1.1[a]	55 ± 5	49 ± 1.0[a]
C. glabrata	44.7 ± 8	48.3 ± 3.5	36.3 ± 1.5
C. krusei	49.3 ± 1.1	48 ± 2	15 ± 1

[a] Taken from Ref. [37].

Table 3
Minimum inhibitory concentrations (MICs) of $ZnCl_2$, phen, the zinc complex and fluconazole as positive control against selected fungal strains. MIC values in μg mL^{-1}.

	$ZnCl_2$	Phen	Zinc complex	Fluconazole
C. albicans	1500	3[a]	6	>375[a]
C. albicans ATCC	1500	3	6	>375
C. parapsilosis	750	12	12	3
C. parapsilosis ATCC	750	12[a]	12	6[a]
C. tropicalis	750	12[a]	12	1.5[a]
C. glabrata	1500	6	6	47
C. krusei	1500	6	12	47

[a] Taken from Ref. [37].

antifungal activity of the [Cu(o-phen) (cnge)(H_2O)(NO_3)$_2$] complex. The antifungal activity displayed by the copper complex resulted lower (higher MIC values) than that of the zinc complex for *C. albicans*, *C. parapsilosis* ATCC and *C. tropicalis*.

4.3. Analysis of the post antifungal effect (PAFE)

The values of PAFEs are given in Table 4. A PAFE of 20 min or less was considered insignificant owing to the limitations of the testing procedure and a value of zero has been assigned in this case [36]. The PAFEs of the metal and the ligand cnge were not determined because they exerted low to moderate activity against all strains of Candida and the determination of the PAFEs values could not be performed without the MIC values.

The determinations showed that 2× MIC concentrations of the ligand phen caused measurable PAFEs values on *C. albicans* ATCC, *C. parapsilosis*, *C. glabrata* and *C. krusei*. The observed order of PAFEs of the ligand phen was *C. glabrata* > *C. krusei* > *C. albicans* ATCC > *C. parapsilosis*.

For the zinc complex, the observed PAFEs order was *C. krusei* > *C. glabrata* > *C. albicans* ATCC > *C. tropicalis* > *C. parapsilosis* ATCC > *C. albicans*. It is interesting to note that the complex exhibited longer PAFEs than the ligand phen in all cases except in the strain in which no post antifungal effect has been found, *C. parapsilosis*. The enhanced PAFE values upon complexation can be explained on the bases of Tweedy's chelation theory. In this theory, chelation reduces the polarity of the central metal atom because of the partial sharing of its positive charge with the ligand. Further, it increases the delocalization of π-electrons over whole chelate ring and enhances the lipophilicity of the complexes [45,46]. This increased lipophilicity of the complex could be responsible for the longer PAFE because the complex could remain more time in the lipidic components of the cell membrane. The increased values of PAFEs upon complexation are relevant in a clinical perspective because the presence of this effect may be an important consideration in designing antifungal dosage regimens. A prolonged PAFE should allow extension of antifungal dosing intervals beyond the time that antifungal concentrations fall below the MIC [36].

To our knowledge, there are no reports of PAFE values for other zinc complexes, so we have performed the comparison of these values with those reported previously, and determined under similar experimental conditions, for some anifungal agents like Nystatin [47] and Amphotericin B [48,49] (see Table 4). It can be seen that the Zn complex displayed higher PAFEs against *C. albicans* ATCC. On the other hand, 5-Fluorocytosine exerted measurable PAFEs on *C. albicans* [48,50], while Fluconazole exerted no relevant PAFEs on this fungal strain [48,50]. Ketoconazole exerted a measurable PAFE on *C. albicans* at values of 4× MIC [50], but not on *C. albicans* ATCC at values of 1× MIC [48]. The PAFE of the zinc complex on *C. albicans* and *C. albicans* ATCC resulted similar to that of 5-Fluorocytosine at values of 1× MIC [48], but lower at values higher than 2× MIC [48,50]. Besides, the PAFEs values reported for the [Cu(o-phen) (cnge) (H_2O) (NO_3)$_2$] [37] complex resulted higher for *C. albicans* and *C. parapsilosis* ATCC than those of the zinc complex, but not for *C. tropicalis*.

The results of this study indicated that the complexation with zinc could enhance the PAFE values of the phenanthroline even with a better efficiency than those of some antifungal agents.

4.4. Toxicological assays

The Ames *S. typhimurium* assay has been used to identify substances that can produce genetic damage that leads to gene mutations. The test uses *Salmonella* strains with preexisting mutations that are not capable to synthesize histidine, and then are not able to grow or form colonies in its absence. Compounds with mutagenic potential may restore the genes function (reversion assay). Consequently, a positive test indicates that the compound is mutagenic and therefore may act as a carcinogen. A sample was considered positive when the mutagenic index (MI) was equal or greater than 2 for at least one of the tested doses and if it had a reproducible dose–response curve [41]. It can be seen in Table 5 that the ligand phen and the zinc complex did not exert mutagenic action on the tested strains.

Table 4
Post-antifungal effect (PAFE) of the ligand phen and the zinc complex against fungal strains. PAFE values in h. PAFE values of Nystatin [47] and Amphotericin B [48,49] have been included for comparative purposes.

	Phen	Zinc complex	Nystatin[b] or Amphotericin B[c,d]
C. albicans	0[a]	0.55 ± 0.07	6.85[b] > 12[c]
C. albicans ATCC	2.15 ± 0.49	2.35 ± 0.49	0.80[d]
C. parapsilosis	1.75 ± 0.35	0	15.17[b]
C. parapsilosis ATCC	0[a]	0.75 ± 0.35	
C. tropicalis	0[a]	1.85 ± 0.21	12.73[b]
C. glabrata	2.90 ± 0.14	3.80 ± 0.28	8.51[b]
C. krusei	2.75 ± 0.35	5.85 ± 0.21	11.58[b]

[a] PAFEs determined at values of 2× MIC [37].
[b] PAFEs of Nystatin determined at values of 1× MIC [47].
[c] PAFE of Amphotericin B determined at values of 2× MIC [49].
[d] PAFE of Amphotericin B determined at values of 1× MIC [48].

Table 5
Induction of His+ revertants (Rev) in *Salmonella typhimurium* (TA98 and TA100) by the ligand phen and the zinc complex without metabolic activation (S9 mix).

	Concentration (μg/plate)	*S. typhimurium* TA98		*S. typhimurium* TA100	
		Rev/plate[a]	MI[b]	Rev/plate[a]	MI[b]
Strain control		20 ± 4	–	128 ± 16	–
Phen	47	16 ± 4	0.80	48 ± 3	0.40
	24	26 ± 1	1.30	129 ± 35	1.00
	12	16 ± 1	0.80	156 ± 1	1.20
Zinc complex	47	23 ± 5	1.15	88 ± 12	0.70
	24	27 ± 1	1.35	146 ± 8	1.10
	12	26 ± 3	1.30	167 ± 46	1.30

[a] Number of revertants/plate: mean of two independent experiments ± SD.
[b] MI: mutagenic index (number of His+ induced in the sample/number of spontaneous His+ in the negative control).

Table 6
Mortality obtained and estimate of LC50 values using *Artemia salina* test.

	Concentration (μg mL^{-1})	Mortality (%)	LC50 value (μg mL^{-1})
Phen	188	96.4	93.7
	94	69.2	
	47	14.8	
	24	7.1	
	12	3.8	
Zinc complex	188	3.8	–
	94	0	
	47	0	
	24	0	
	12	0	

The mutagenic index was <2 in all the cases and this demonstrate that the tested substances could not induce an increase in the number of revertants. These results indicated that both phen and the complex did not induce frameshift mutations (*S. typhimurium* TA98) or base-pair substitution mutations (*S. typhimurium* TA100) at the tested concentrations. C. Deegan et al. also reported non-mutagenic action of phen on *S. typhimurium* TA 98 and TA102 [51].

The *A. salina* L. test is useful for the screening of novel drugs in order to predict their toxicity and has shown a good correlation ($r = 0.85$ $p < 0.05$) with the assays in mice, suggesting that the brine shrimp bioassay is a useful alternative model [52]. The mortality of brine shrimp for every concentration of the ligand phen and the zinc complex is shown in Table 6.

For the ligand phen, the mortality increased in a dose–response manner. This linearity in the dose–effect relationship allowed us to determine the median lethal concentration LC50 value (93.70 μg mL^{-1}), which is the dose required to kill half of the members of the tested population. On the other hand, dead nauplii were not observed for the zinc complex at the tested concentrations (except at 188 μg mL^{-1}). This important finding indicated that the toxicity of the ligand phen decreased after complexation. In this context, the zinc complex could be safer than the ligand to be used as antifungal agent.

5. Conclusions

The DFT-optimized structures converged successfully to a structure, which is in good agreement with the experimental one determined by the X-ray diffraction method. The total theoretical IR and Raman spectra averaged over the two complexes and weighted by their relative stabilities, resulted in a good agreement with the experimental vibrational spectra.

The complexation increases the antifungal activity of the metal and the ligand cnge, but slightly decreases the antifungal activity of the ligand phen against *C. albicans*, *C. albicans* ATCC and *C. krusei*. The ligand phen and the zinc complex showed higher activity than fluconazole against *C. albicans*, *C. albicans* ATCC, *C. glabrata* and *C. krusei*. The complexation also increases the PAFE in all cases, except for *C. parapsilosis*. The zinc complex exhibited longer PAFEs against some strains of Candida than some conventional antifungal agents.

The ligand phen and the zinc complex were non mutagenic agents at the tested concentrations. Nevertheless, a decrease in the acute toxicity of the ligand after complexation was observed and this could indicate that the zinc complex can be safer than phenanthroline to be used as antifungal agent.

In this context, we can conclude that some biological properties have been modified upon complexation with zinc and this complexation may provide a promising strategy for the development of novel and more secure drugs with antifungal activity.

Acknowledgments

This work was supported by UNLP, CICPBA (PICyT 813/13), ANPCyT (PICT-2013-0569), UNCAUS, CONICET and CIN. EGF and NBO are members of the Carrera del Investigador of CONICET. PAMW is a member of the Carrera del Investigador of CICPBA, Argentina. JJMM and CAT are fellowship holders from CONICET. WSA is a fellowship holder from CIN.

Appendix A. Supplementary data

Supplementary data related to this article can be found at http://dx.doi.org/10.1016/j.molstruc.2015.07.061.

References

[1] A.S. Batsanov, P. Hubberstey, C.E. Russell, P.H. Waltin, J. Chem. Soc. Dalton Trans. (1997) 2667–2672.
[2] L.M.D.R.S. Martins, J.J.R. Fraústo da Silva, A.J.L. Pombeiro, R.A. Henderson, D.J. Evans, F. Benetollo, G. Bombieri, R.A. Michelin, Inorg. Chim. Acta 291 (1999) 39–48.
[3] L. A. Sheludyakova, the late E. V. Sobolev, A. V. Arbuznikov, E. B. Burgina, L. I. Kozhevina, J. Chem. Soc. Faraday Trans. 93 (1997) 1357–1360.
[4] P. Ray, Chem. Rev. 61 (1960) 313–359.
[5] R.L. Dutta, A.M. Singh, J. Indian Chem. Soc. 52 (1975) 1000–1001.

[6] W.K. Baker Jr., M. Daniels, J. Inorg. Nucl. Chem. 25 (1963) 1194–1196.
[7] P.A.M. Williams, E.G. Ferrer, N. Baeza, O.E. Piro, E.E. Castellano, E.J. Baran, Z. Anorg, Allg. Chem. 631 (2005) 1502–1506.
[8] A. Bencini, V. Lippolis, Coord. Chem. Rev. 254 (2010) 2096–2180.
[9] M.A. Zoroddu, S. Zanetti, R. Pogni, R. Basosi, J. Inorg. Biochem. 63 (1996) 291–300.
[10] A.S. Prasad, J. Am. Coll. Nutr. 15 (1996) 113–120.
[11] A.A. Recio Despaigne, F.B. Da Costa, O.E. Piro, E.E. Castellano, S.R.W. Louro, H. Beraldo, Polyhedron 38 (2012) 285–290.
[12] A. Berahou, A. Auhmani, N. Fdil, A. Benharref, M. Jana, C.A. Gadhi, J. Ethnopharmacol. 112 (2007) 426–429.
[13] S.B. Kalia, G. Kaushal, M. Kumar, S.S. Cameotra, A. Sharma, M.L. Verma, S.S. Kanwar, Braz. J. Microbiol. 40 (2009) 916–922.
[14] M.O. Agwara, P.T. Ndifon, N.B. Ndosiri, A.G. Paboudam, D.M. Yufanyi, A. Mohamadou, Bull. Chem. Soc. Ethiop. 24 (2010) 383–389.
[15] J. Pasquet, Y. Chevalier, J. Pelletier, E. Couval, D. Bouvier, M.A. Bolzinger, Colloids Surf. A Physicochem. Eng. Asp. 457 (2014) 263–274.
[16] A.M.K. Raja Balan, R.F.N. Ashok, M. Vasanthi, R. Prabu, A. Paulraj, Inorg. Chim. Acta 408 (2013) 103–108.
[17] K. Alomar, A. Landreau, M. Kempf, M.A. Khan, M. Allain, G. Bouet, J. Inorg. Biochem. 104 (2010) 397–404.
[18] V. Kumar, T. Ahamad, N. Nishat, Eur. J. Med. Chem. 44 (2009) 785–793.
[19] A. Mastrolorenzo, A. Scozzafava, C.T. Supuran, Eur. J. Pharm. Sci. 11 (2000) 99–107.
[20] J. Sheikh, H. Juneja, V. Ingle, P. Ali, T. Ben Hadda, J. Saudi Chem. Soc. 17 (2013) 269–276.
[21] B. Čobeljić, A. Pevec, I. Turel, M. Swart, D. Mitić, M. Milenković, I. Marković, M. Jovanović, D. Sladić, M. Jeremić, K. Anđelković, Inorg. Chim. Acta 404 (2013) 5–12.
[22] M. Montazerozohori, S. Zahedi, A. Naghiha, M. Montazer Zohour, Mater. Sci. Eng. C 35 (2014) 195–204.
[23] B. Holló, J. Magyari, V. Živković-Radovanović, G. Vučković, Z.D. Tomić, I. Miklós Szilágyi, G. Pokol, K. Mészáros Szécsényi, Polyhedron 80 (2014) 142–150.
[24] L.L. López Tévez, M.S. Islas, J.J. Martínez Medina, M. Diez, O.E. Piro, E.E. Castellano, E.G. Ferrer, P.A.M. Williams, J. Coord. Chem. 65 (2012) 2304–2318.
[25] W. Kohn, L.J. Sham, Phys. Rev. 140 (1965) A1133–A1138.
[26] P. Hohenberg, W. Kohn, Phys. Rev. 136 (1964) B864–B871.
[27] R.G. Parr, W. Yang, Density Functional Theory of Atoms, Molecules, Oxford University Press, Clarendon Press, Oxford; New York, 1989.
[28] M.J. Frisch, G.W. Trucks, H.B. Schlegel, G.E. Scuseria, M.A. Robb, J.R. Cheeseman, G. Scalmani, V. Barone, B. Mennucci, G.A. Petersson, H. Nakatsuji, M. Caricato, X. Li, H.P. Hratchian, A.F. Izmaylov, J. Bloino, G. Zheng, J.L. Sonnenberg, M. Hada, M. Ehara, K. Toyota, R. Fukuda, J. Hasegawa, M. Ishida, T. Nakajima, Y. Honda, O. Kitao, H. Nakai, T. Vreven, J.A. Montgomery Jr., J.E. Peralta, F. Ogliaro, M. Bearpark, J.J. Heyd, E. Brothers, K.N. Kudin, V.N. Staroverov, T. Keith, R. Kobayashi, J. Normand, K. Raghavachari, A. Rendell, J.C. Burant, S.S. Iyengar, J. Tomasi, M. Cossi, N. Rega, J.M. Millam, M. Klene, J.E. Knox, J.B. Cross, V. Bakken, C. Adamo, J. Jaramillo, R. Gomperts, R.E. Stratmann, O. Yazyev, A.J. Austin, R. Cammi, C. Pomelli, J.W. Ochterski, R.L. Martin, K. Morokuma, V.G. Zakrzewski, G.A. Voth, P. Salvador, J.J. Dannenberg, S. Dapprich, A.D. Daniels, O. Farkas, J.B. Foresman, J.V. Ortiz, J. Cioslowski, D.J. Fox, Gaussian 09, Revision B.01, Gaussian, Inc, Wallingford CT, 2010.
[29] A.D. Becke, J. Chem. Phys. 98 (1993) 5648–5652.
[30] M.E. Casida, C. Jamorski, K.C. Casida, D.R. Salahub, J. Chem. Phys. 108 (1998) 4439–4449.
[31] D. Rappoport, F. Furche, J. Chem. Phys. 133 (2010) 134105-1–134105-11. http://www.castl.uci.edu/sites/default/files/images/Rappoport_JCP_133_Property-optimzed%20Gaussian_2010.pdf.
[32] A.V. Arbuznikov, L.A. Sheludyakova, E.B. Burgina, Chem. Phys. Lett. 240 (1995) 239–244.
[33] M.S. Islas, C.A. Franca, S.B. Etcheverry, E.G. Ferrer, P.A.M. Williams, Vib. Spectrosc. 62 (2012) 143–151.
[34] D.R. Flower, J. Mol. Graph. Modell. 17 (1999) 238–244.
[35] J.D. Gans, D. Shalloway, J. Mol. Graph. Modell. 19 (2001) 557–559.
[36] D.L. Rescott, D.E. Nix, P. Holden, J.J. Schentag, Antimicrob. Agents Chemother. 32 (1988) 450–453.
[37] J.J. Martínez Medina, M.S. Islas, L.L. López Tévez, E.G. Ferrer, N.B. Okulik, P.A.M. Williams, J. Mol. Struct. 1058 (2014) 298–307.
[38] J.C.A. Tanaka, C.C. da Silva, A.J.B. de Oliveira, C.V. Nakamura, B.P. Dias Filho, Braz. J. Med. Biol. Res. 39 (2006) 387–391.
[39] A.A. Aliero, A.D. Ibrahim, Antibiotic resistance and the prospects of medicinal plants in the treatment of Salmonellosis, in: Y. Kumar (Ed.), Salmonella: a Diversified Superbug, In Tech, Open Access Company, Croatia, Europe, 2012, pp. 65–90 (Chapter 4).
[40] A. Bacchi, M. Carcelli, P. Pelagatti, C. Pelizzi, G. Pelizzi, F. Zani, J. Inorg. Biochem. 75 (1999) 123–133.
[41] D.M. Maron, B.N. Ames, Mutat. Res. 113 (1983) 173–215.
[42] B.N. Meyer, N.R. Ferrigni, J.E. Putnam, L.B. Jacobsen, D.E. Nichols, J.L. McLaughlin, Planta Med. 45 (1982) 31–34.
[43] L. Lewan, M. Andersson, P. Morales-Gomez, Altern. Lab. Anim. 20 (1992) 297–301.
[44] J.M. Alía, H.G.M. Edwards, F.J. García Navarro, J. Mol. Struct. 597 (2001) 49–55.
[45] S. Chandraleka, K. Ramya, G. Chandramohan, D. Dhanasekaran, A. Priyadharshini, A. Panneerselvam, J. Saudi Chem. Soc. 18 (2014) 953–962.
[46] M.N. Patel, P.A. Dosi, B.S. Bhatt, V.R. Thakkar, Spectrochim. Acta Part A 78 (2011) 763–770.
[47] A.N. Ellepola, L.P. Samaranayake, J. Oral Pathol. Med. 28 (1999) 112–116.
[48] M.T. García, M.T. Llorente, F. Mínguez, J. Prieto, J. Infect. 45 (2002) 263–267.
[49] E.J. Ernst, M.E. Klepser, M.A. Pfaller, Antimicrob. Agents Chemother. 44 (2000) 1108–1111.
[50] A.N. Ellepola, L.P. Samaranayake, Oral Dis. 4 (1998) 260–267.
[51] C. Deegan, M. McCann, M. Devereux, B. Coyle, D.A. Egan, Cancer Lett. 247 (2007) 224–233.
[52] A. Lagarto Parra, R. Silva Yhebra, I. Guerra Sardiñas, L. Iglesias Buela, Phytomedicine 8 (2001) 395–400.